Acta Cryst. (1993). A**49**, 576–585

On the Solution of the Phase Problem in Quasiperiodic Crystals

BY MARKO VUKOBRAT JARIĆ AND SHI-YUE QIU*

Center for Theoretical Physics, Texas A&M University, College Station, TX 77843-4242, *USA*

(*Received* 12 *March* 1992; *accepted* 16 *November* 1992)

Abstract

A general method is presented to solve the phase problem and determine density maps of quasiperiodic crystals for which periodic crystals approximating them are known. The method is first successfully tested on certain icosahedral quasiperiodic tilings and then applied to X-ray and neutron diffraction data of $i(Al_{0.570}Cu_{0.108}Li_{0.322})$. It yields the first direct model-independent density maps of an icosahedral quasicrystal. The obtained phases are found to be in good agreement with the existing structural models fitted to the same diffraction data.

Introduction

Diffraction experiments have been the most common probe of the structure of solids for nearly a century. The structure of a solid can be described in terms of an average structure or, more generally, in terms of an *ideal atomic structure* and fluctuations around it. The *average structure* of a solid can often be represented by an appropriately ensemble-averaged density of scatterers $\rho(\mathbf{r})$ or, equivalently, by its Fourier transform (structure factor) $F(\mathbf{q}) \equiv |F(\mathbf{q})| \exp[i\theta(\mathbf{q})]$. However, even ideally, a diffraction experiment yields only the magnitude $|F(\mathbf{q})|$. Therefore, the determination of the average structure of a solid can be reduced to the determination of the phase $\theta(\mathbf{q})$.

This so-called 'phase problem' has been solved for periodic crystals by Hauptman and Karle who received the 1985 Nobel Prize in Chemistry for their solution (Hauptman, 1986; Karle, 1986). Their statistical method simultaneously solves the phase problem and determines the ideal atomic structure. Although this method could be extended to the incommensurate crystals with a well defined underlying periodic atomic structure, an all-encompassing method has not been found for general quasiperiodic crystals, such as those with noncrystallographic symmetries. Many quasicrystals may be examples of such more general quasiperiodic crystals (Steinhardt & Ostlund, 1987).†

In this article, we present a method to solve the phase problem for the class of quasiperiodic crystals for which periodic crystals approximating them exist and have a known atomic structure (*i.e.* their phase problem is solved). Besides the phases, the method also yields the absolute scale for the diffraction intensities (and structure factors), which is extremely difficult to obtain experimentally and, hence, often unavailable. Thus, while the method does not address the question of the ideal atomic structure of a quasiperiodic crystal, it solves the problem of the construction of its average structure.

This article completes our earlier conference reports on the work in progress (Qiu & Jarić, 1989, 1990; Jarić & Qiu, 1990, 1991). We shall first demonstrate that this method works extremely well in the case of certain icosahedral quasiperiodic tilings called Ammann tilings (Mackay, 1981; Tang, 1991). Then, we shall illustrate our method by solving the phase problem for both X-ray and neutron diffraction data of the $i(Al_{0.570}Cu_{0.108}Li_{0.322})$ quasicrystal obtained by de Boissieu, Janot, Dubois, Audier & Dubost (1991). It will be assumed that the average structure of $i(Al_{0.570}Cu_{0.108}Li_{0.322})$ is quasiperiodic. We shall also determine the structure factors in absolute units, as given in Table 1, and we shall construct the first direct (*i.e.* independent of a specific atomic structure model) quasiperiodic density maps of a quasicrystal. Examples of these density maps, shown in Fig. 1, will be briefly discussed. A complete analysis of the implications of our results for the $i(Al_{0.570}Cu_{0.108}Li_{0.322})$ quasicrystal necessitates a more extensive study and will be presented elsewhere.

Quasiperiodic crystals

To lowest order, the scattering intensity $I(\mathbf{q})$ measured in a diffraction experiment is proportional to $\langle |F_\mu(\mathbf{q})|^2 \rangle$, where $\langle \cdot \rangle$ denotes thermal (ensemble) averaging and the subscript μ denotes density of scatterers before averaging.† To extract $F(\mathbf{q}) \equiv \langle F_\mu(\mathbf{q}) \rangle$, we invoke $|F(\mathbf{q})|^2 = \langle |F_\mu(\mathbf{q})|^2 \rangle$, which has been recently shown (Jarić & Nelson, 1988) for quasiperiodic crystals to be correct to order $O(1/N)$,

* Present address: Department of Physics, Iowa State University, Ames, IW 50011, USA.

† We assume the empirical definition of a quasicrystal: a material experimentally characterized by sharp diffraction peaks (coherence length of at least several hundred ångströms) and by a noncrystallographic symmetry, such as icosahedral, octagonal, decagonal or dodecagonal.

† For simplicity, we shall focus here only on the case of thermal disorder although a large class of disorder types can be treated similarly. The solid will be assumed clamped, that is, its center of mass and orientation fixed.

0108-7673/93/030576-10$06.00

Table 1. *Fourier transforms of the scatterer densities in* $i(Al_{0.570}Cu_{0.108}Li_{0.322})$, *for X-rays* ($F_{\mathbf{Q}}^{X\text{-}ray}$) *and neutrons* ($F_{\mathbf{Q}}^{neutron}$), *reconstructed from the diffraction data by de Boissieu et al.* (1991)

The icosahedral indexing, column **Q**, follows Jarić (1986, 1987).

Q	$\lvert\mathbf{Q}^{\perp}\rvert$ (Å^{-1})	$\lvert\mathbf{Q}\rvert$ (Å^{-1})	$F_{\mathbf{Q}}^{X\text{-}ray}$ ($\times10^{-2}$ e Å^{-3})	$F_{\mathbf{Q}}^{neutron}$ ($\times10^{-7}$ Å^{-2})	**Q**	$\lvert\mathbf{Q}^{\perp}\rvert$ (Å^{-1})	$\lvert\mathbf{Q}\rvert$ (Å^{-1})	$F_{\mathbf{Q}}^{X\text{-}ray}$ ($\times10^{-2}$ e Å^{-3})	$F_{\mathbf{Q}}^{neutron}$ ($\times10^{-7}$ Å^{-2})
000000	0.000	0.000	69.67	12.99	442002	0.499	5.535	7.62	3.82
41441$\bar{1}$	0.083	6.275	2.91	3.97	11432$\bar{3}$	0.499	5.535	−1.77	
1121$\bar{1}\bar{1}$	0.147	2.632	−11.16		533112	0.520	6.129	−2.63	
332002	0.154	4.478	15.72	4.11	0021$\bar{1}\bar{1}$	0.534	2.263	1.68	
4264$\bar{1}\bar{2}$	0.175	7.709		6.35	2242$\bar{2}\bar{1}$	0.556	5.017	3.31	
52650$\bar{2}$	0.181	8.518		2.19	0042$\bar{2}\bar{3}$	0.556	5.017	4.75	1.98
1142$\bar{2}\bar{3}$	0.213	5.194	4.00	3.59	4441$\bar{1}$0	0.558	6.188	2.10	
3352$\bar{2}\bar{1}$	0.218	6.333	0.97		2252$\bar{2}\bar{3}$	0.558	6.188	1.48	
221001	0.250	2.768	17.31	3.54	0043$\bar{3}\bar{4}$	0.558	6.188	1.25	
4353$\bar{1}\bar{1}$	0.263	6.858		−1.47	1131$\bar{1}\bar{2}$	0.590	3.575	−3.22	−1.39
5551$\bar{1}$1	0.267	7.756		−3.41	2043$\bar{1}\bar{2}$	0.591	5.090	2.57	
4363$\bar{2}\bar{2}$	0.267	7.756		2.15	202310	0.623	3.676	1.58	
2231$\bar{1}$0	0.289	3.819	5.49	3.87	001100	0.653	1.057	2.44	1.08
2242$\bar{2}\bar{2}$	0.293	5.264	17.71	7.49	4044$\bar{1}\bar{2}$	0.659	6.363	1.77	
3341$\bar{1}$0	0.293	5.264		−1.33	0$\bar{1}$121$\bar{2}$	0.670	2.836	−1.86	
0064$\bar{4}\bar{6}$	0.308	8.956		3.60	333001	0.671	4.601	−0.97*	
2252$\bar{2}\bar{2}$	0.328	5.886		5.88	1132$\bar{2}\bar{3}$	0.671	4.601	−2.38	
443002	0.328	5.886	9.27	5.83	3341$\bar{1}$1	0.687	5.301	−1.58	
4154$\bar{0}\bar{2}$	0.331	6.911		2.20	3341$\bar{1}\bar{1}$	0.687	5.301	−1.25	
100110	0.350	1.481	9.05	3.65	1153$\bar{3}\bar{3}$	0.689	6.421	−1.94	
2231$\bar{1}\bar{1}$	0.353	3.914		−1.61	1121$\bar{1}\bar{2}$	0.699	2.963	1.12†	
3331$\bar{1}$0	0.382	4.717	−4.98	−1.69	222000	0.699	2.963	2.17	
1043$\bar{2}\bar{4}$	0.385	5.947	4.91	2.15	1111$\bar{1}$0	0.741	1.820	−2.63	−0.94
636400	0.394	8.646		2.20	333002	0.757	4.834	−2.63	−1.29
0011$\bar{1}\bar{1}$	0.404	1.710	−2.91	−1.82	1111$\bar{1}\bar{1}$	0.768	2.011	−2.96	−1.33
3352$\bar{2}\bar{2}$	0.412	6.504		1.77	2221$\bar{1}$1	0.782	3.312	−3.12	−1.68
222001	0.430	3.139	13.82	5.85	0031$\bar{1}\bar{2}$	0.782	3.312	−2.10	
3331$\bar{1}$1	0.432	4.749	−6.67	−3.60	2221$\bar{1}\bar{1}$	0.782	3.312	−0.97	
1142$\bar{2}\bar{2}$	0.432	4.749	6.67	2.22	1143$\bar{1}\bar{2}$	0.783	4.909	−1.94	
3342$\bar{1}$0	0.456	5.469	2.24	1.45	1031$\bar{1}\bar{2}$	0.808	3.421	−1.94	
2221$\bar{1}$0	0.475	3.253	5.68	1.94	201200	0.844	2.497	−2.02	
1131$\bar{1}\bar{1}$	0.475	3.253	−8.87	−3.64	211200	0.868	2.640	−2.17	
4254$\bar{0}\bar{2}$	0.482	7.068		2.93	1011$\bar{1}$0	0.924	1.495	−2.50	
332001	0.497	4.185	0.79	1.33	2022$\bar{1}\bar{1}$	0.957	3.146	−2.69	
1132$\bar{2}\bar{2}$	0.497	4.185	3.17	1.35	10200$\bar{1}$	1.132	1.831	−1.94	

* The phase here is opposite from that determined in the structure model of de Boissieu *et al.* (1989).
† The phase here is opposite from that determined in the structure model of de Boissieu *et al.* (1991).

where N is the total number of scatterers. Therefore, in the thermodynamic limit $N\to\infty$, the magnitude $|F(\mathbf{q})|\sim[I(\mathbf{q})]^{1/2}$ can be directly measured, at least in principle, but additional information is still needed to determine the phase $\theta(\mathbf{q})$.

By definition, the Fourier transform of a quasiperiodic crystal density is discrete, $F(\mathbf{q})=\sum_{\mathbf{Q}\in\{\mathbf{Q}\}}F_{\mathbf{Q}}\delta(\mathbf{q}-\mathbf{Q})$. Its reciprocal lattice $\{\mathbf{Q}\}$ is generated by all integral linear combinations of D vectors ($3<D<\infty$) that span the three-dimensional 'physical' space. Periodic crystals can be considered as a special case ($D=3$) of this definition. This definition of quasiperiodic crystals does not exclude the presence in the diffraction pattern of a diffuse background $O(1/N)$ relative to the Bragg peaks.

The indexing problem, *i.e.* the determination of the reciprocal lattice $\{\mathbf{Q}\}$ of a quasiperiodic crystal, can be solved by the location of the set of positions of experimentally observed diffraction spots (Cahn, Shechtman & Gratias, 1986). For a periodic crystal, this fixes its unit cell and, from the stoiochiometry and overall density, the number and kinds of atoms it contains. Since this number is finite (typically not very large), the class of possible crystal structures can be parametrized with a *finite* number of parameters (*e.g.* ideal positions and thermal-motion ellipsoids of the atoms within a unit cell). Such *a priori* finite parametrization, which is an essential ingredient of the Hauptman–Karle method, is not possible in the general case of quasiperiodic crystals, thus an alternative method is needed. The basic idea of our approach is to provide constraints on the phases by relating a quasiperiodic crystal to a *similar* periodic crystal.

Although our approach can be fully formulated in the physical space, we find a higher-dimensional approach conceptually simpler (Besicovitch, 1932; Bohr, 1947; Bak, 1986). In this approach, a quasiperiodic density $\rho(\mathbf{r})$ is viewed as an (irrational) three-dimensional cut through a D-dimensional periodic (hyper)crystal density $\bar{\rho}(\bar{\mathbf{r}})$. That is, $\rho(\mathbf{r})=\bar{\rho}(\mathbf{r},\mathbf{r}^{\perp}=0)$, where the $D-3$ components of $\bar{\mathbf{r}}$ along the inner space (orthogonal complement to the physical space) are denoted by $\mathbf{r}^{\perp}$. This is illustrated in Fig. 2(a), where the physical space is one dimensional and the hypercrystal is ($D=2$)-dimensional. The

'irrationality' of the cut means that the cut is not parallel to any of the hypercrystal planes. Consequently, a cut at any other $\mathbf{r}^{\perp} \neq 0$ would result in an equivalent (experimentally indistinguishable) quasiperiodic density.

Another consequence of the irrationality of the cut is that to each reciprocal-lattice vector $\mathbf{Q}$ there corresponds a unique reciprocal-hyperlattice vector $\bar{\mathbf{Q}} \equiv \mathbf{Q}, \mathbf{Q}^{\perp})$. This is illustrated in Fig. 2(*b*), in which we also represent the Fourier transform in the reciprocal hyperspace where $\bar{F}_{\bar{\mathbf{Q}}} \equiv F_{\mathbf{Q}}$. It should be noted that $\mathbf{Q}^{\perp}$, and thus F, cannot be generally represented by a smooth function of $\mathbf{Q}$. Therefore, we shall sometimes view F as a smooth function of the variables $\mathbf{Q}$ and $\mathbf{Q}^{\perp}$.

Since the inner space is a mathematical construction and not even a unique one, it is necessary to specify its characteristic ('unit') length scale $l_{\perp}$. The characteristic length scale l in the physical space is given by a typical interatomic separation in the material, $l \sim v^{1/3}$, where v is the specific volume (volume per atom). Similarly, the characteristic length scale in the inner space can be defined by $l_{\perp} \sim (\bar{v}/v)^{1/(D-3)}$, where $\bar{v}$ denotes volume of the unit cell of the hypercrystal. When expressed in units of $l_{\perp}$, the inner-space lengths will be independent of a particular hypercrystal description used.

Method

A quasiperiodic crystal can be transformed into a periodic crystal by distorting the underlying hypercrystal with a shear $\mathsf{E}^{\perp}$ parallel to the inner space that brings a three-dimensional hypercrystal plane into a parallel orientation with the physical space, as illustrated in Fig. 2(*c*).* This 'rational' shear may be followed by a linear transformation L in the physical space. The resulting periodic crystal structure will

* It has been suggested that some quasiperiodic crystals may undergo a transition that corresponds to a simple displacive distortion of the underlying hypercrystal (Jarić & Mohanty, 1987). It should be emphasized, however, that an *actual* occurrence of such a 'displacive' transition between a quasiperiodic crystal and its periodic counterpart is not a prerequisite for our method.

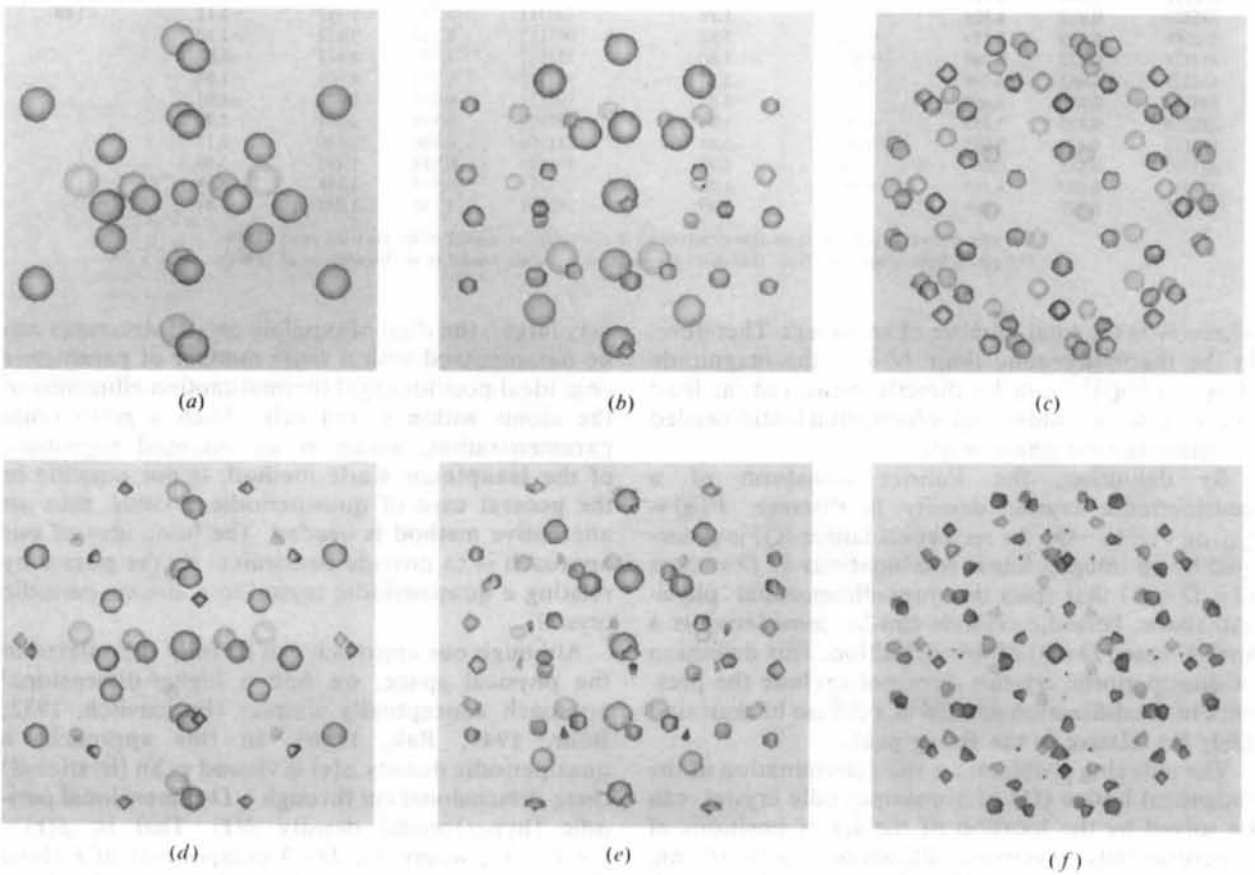

Fig. 1. Surfaces of constant scatterer density in $i(Al_{0.570}Cu_{0.108}Li_{0.322})$ computed from the data in Table 1. For X-rays, the density is 11.9 e Å^{-3} (*a*)-(*c*). For neutrons, the density is -3.17×10^{-5} Å^{-2} or 7.39×10^{-5} Å^{-2} (*d*)-(*f*). The negative density surfaces in (*d*)-(*f*) are those that have no counterpart in (*a*)-(*c*). The figures are centered at the *unique* $53m$ or $\bar{5}m$ symmetry points and shown within spheres of radii 5.6 Å (*a*), (*b*), (*d*), (*e*) or 7.8 Å (*c*), (*f*). Shading is used to indicate depth.

generally depend on the position of the cut, *i.e.* on the value of $\mathbf{r}^{\perp}$. Any other components of a linear transformation of the hypercrystal are a consequence of the inherent redundancy in the hypercrystal description and will not be explicitly considered here.

Associated with the distortion of the hypercrystal is a distortion of its reciprocal hyperlattice. The distorted reciprocal-hyperlattice vectors $\{\bar{\mathbf{Q}}'\}$ are related to the undistorted ones by

$$(\mathbf{Q}'\mathbf{Q}'^{\perp}) = (\mathbf{Q}\mathbf{Q}^{\perp}) \begin{pmatrix} \mathsf{L} & 0 \\ \mathsf{E}^{\perp} & 1 \end{pmatrix}^{-1} \equiv (\mathbf{Q}\mathbf{Q}^{\perp})\bar{\mathsf{L}}^{-1}, \quad (1)$$

where the bold indicates row vectors, $\mathsf{E}^{\perp}$ is a $(D-3)\times 3$ matrix that describes the rational shear and L is a 3×3 matrix that describes the linear distortion in the physical space. A distortion of the reciprocal hyperlattice resulting from a rational shear is illustrated in Fig. 2(*d*). We can see that a reciprocal-lattice vector $\mathbf{Q}'$ now corresponds to infinitely many different reciprocal-hyperlattice vectors $\bar{\mathbf{Q}}'$, each one having a different inner-space component $\mathbf{Q}'^{\perp}$. In this way, the dense set of Bragg peaks of the quasiperiodic crystal collapses into the set of isolated Bragg peaks of the periodic crystal.

We shall call a periodic crystal obtained in the physical space by the above-described construction a 'rational approximant' of the quasiperiodic crystal. Fourier components of its density, $F^{r}_{\mathbf{Q}'}$, are related to the Fourier components of the quasicrystal density by

$$F^{r}_{\mathbf{Q}'} = (\det \mathsf{L})^{-1} \sum_{\mathbf{Q}'^{\perp}} F_{\mathbf{Q}} = (\det \mathsf{L})^{-1} \sum_{\mathbf{Q}'^{\perp}} |F_{\mathbf{Q}}| \exp[i\theta(\mathbf{Q})]. \quad (2)$$

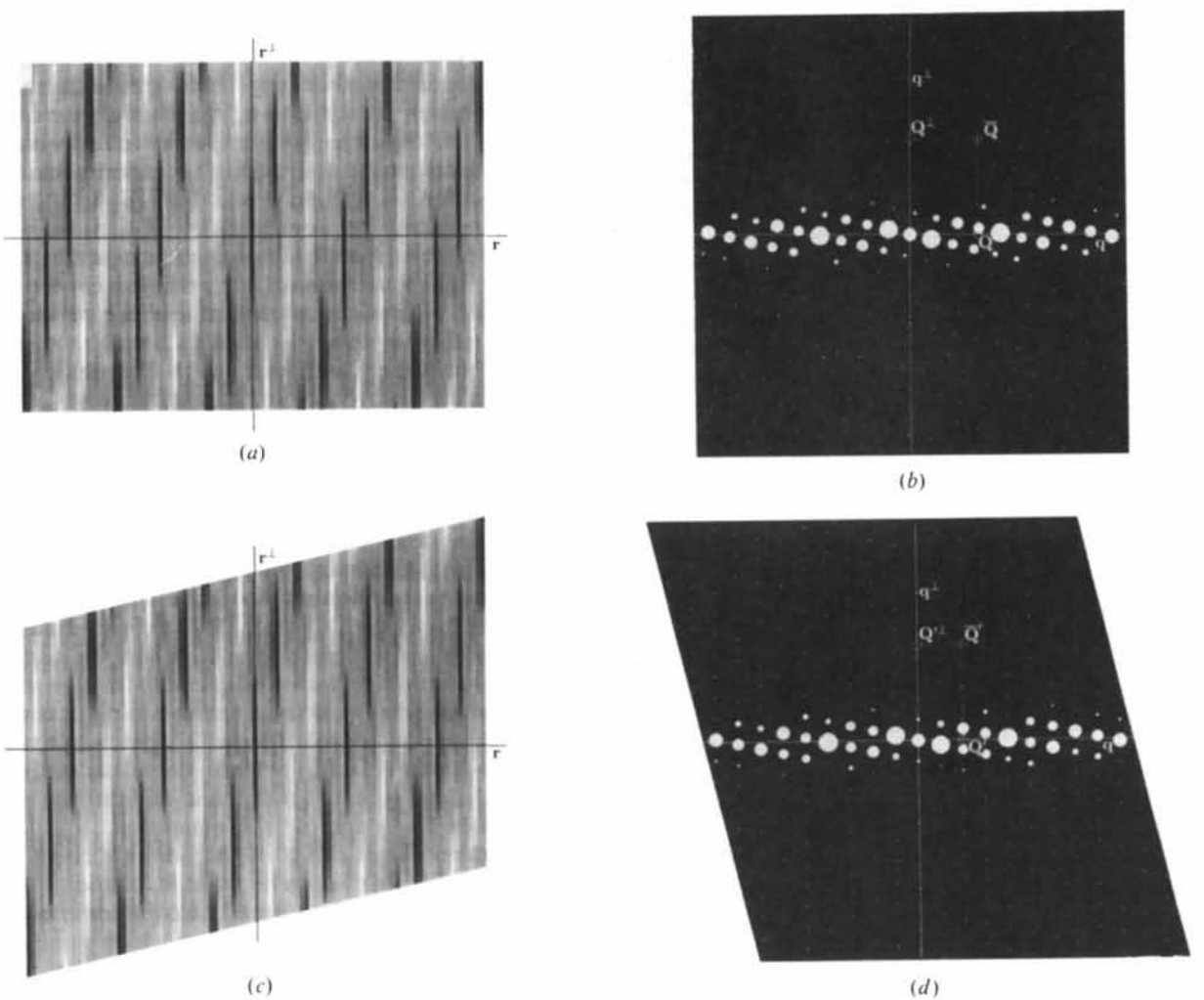

Fig. 2. (*a*), (*c*) A density along the physical space (horizontal line) viewed as a cut through a periodic density in the hyperspace (plane of the figure). In the reciprocal-space representations (*b*), (*d*), the circle diameters are proportional to the square root of the Fourier-series amplitudes. A quasiperiodic physical-space density (*a*), (*b*) is transformed to a periodic one (*c*), (*d*) by a shear in the hyperspace.

An explicit relationship between the different $\mathbf{Q}$ vectors that appear in this equation is given by (1). Since infinitely many different inner-space components $\mathbf{Q}'^{\perp}$ correspond to a given $\mathbf{Q}'$, the sum over $\mathbf{Q}'^{\perp}$ contains infinitely many terms. The phase $\mathbf{Q}'^{\perp}\cdot\mathbf{r}^{\perp}$ associated with the position of the cut is absorbed here into the phase $\theta(\mathbf{Q})$ and can be viewed as a change in $F_{\mathbf{Q}}$ due to a shift of the origin in the hyperspace.

The construction of the rational approximants forms the basis for our method to determine phases $\theta(\mathbf{Q})$ associated with measurable intensities $I_{\mathbf{Q}}$. The fundamental idea of our approach is to relate a rational approximant to a real periodic crystal of known structure and thereby provide a set of constraints on the phases. Since the periodic crystal structure is assumed to be known, both the amplitudes and phases of its Fourier transform $F^{p}_{\mathbf{Q}'}$ are known. Also, $\mathsf{E}^{\perp}$ and L can be determined by comparison of the reciprocal lattice $\{\mathbf{Q}'\}$ of the periodic crystal with the reciprocal lattice $\{\mathbf{Q}\}$ of the quasiperiodic one. Furthermore, except for the usually undetermined scale factor s, $|F_{\mathbf{Q}}|$ equals the measurable value $I_{\mathbf{Q}}^{1/2}$. Thus, by equating $F^{p}_{\mathbf{Q}'}$ with $F'_{\mathbf{Q}'}$, (2) provides the required constraints on the phases $\theta(\mathbf{Q})$.

However, these constraints cannot be considered to be strict. Clearly, the sum in (2) is necessarily truncated since only a finite, typically small, number of intensities entering the sum are experimentally observable. Similarly, there is always an uncertainty $\sigma_{\mathbf{Q}}$, experimentally introduced in the measurement of the diffraction intensities. Moreover, the observed periodic crystal and the constructed rational approximant, although similar, are not expected to be identical in general. For example, a small distortion within the unit cell, in addition to the overall linear distortion of the hypercrystal, may be necessary.

Furthermore, a quasicrystal density will generally include Debye–Waller-like factors $\exp(-\mathbf{Q}^{\perp}\mathsf{B}^{\perp}\mathbf{Q}^{\perp})$, where the $(D-3)\times(D-3)$ matrix $\mathsf{B}^{\perp}$ is the inner-space analog of a thermal-motion ellipsoid (Jarić & Nelson, 1988; Elser, 1985*a*). Physically, $\mathsf{B}^{\perp}$ is a measure of the average fraction of atoms rearranged by phason displacements. Thus, it is expected that $|\mathsf{B}^{\perp}|^{1/2}/l_{\perp}$ would not be greater than several percent (it should certainly not exceed 100%). Such Debye–Waller factors are carried over to a rational approximant but may be inappropriate for the associated periodic crystal. Also, the usual Debye–Waller factors of the quasiperiodic crystal $\exp(-\mathbf{Q}^{\mathsf{B}}\mathbf{Q})$, carried over to a rational approximant, will only approximately account for the thermal motion in the periodic crystal.

Therefore, before identifying $F^{p}_{\mathbf{Q}'}$ with a particular $F'_{\mathbf{Q}'}$, we shall first multiply $F_{\mathbf{Q}}$ by an overall correction factor $\exp(\bar{\mathbf{Q}}\Delta\bar{\mathsf{B}}\bar{\mathbf{Q}})$, where the $D\times D$ matrix $\Delta\bar{\mathsf{B}}$ is to be treated as a fitting parameter. If thermal fluctuations of the quasiperiodic and periodic crystals are characterized by Debye–Waller factors $\exp(-\bar{\mathbf{Q}}\bar{\mathsf{B}}\bar{\mathbf{Q}})$ and $\exp(-\mathbf{Q}'\mathsf{B}^{p}\mathbf{Q}')$, respectively, then

$$\Delta\bar{\mathsf{B}}\equiv\bar{\mathsf{B}}-\bar{\mathsf{L}}^{-1}\bar{\mathsf{B}}^{p}\bar{\mathsf{L}}^{-1}, \tag{3}$$

where the $D\times D$ matrix $\bar{\mathsf{B}}^{p}$ is defined with only the 3×3 block B^{p} as a nonzero entry. Note that $\Delta\bar{\mathsf{B}}$ has the symmetry of the periodic crystal, which determines its number of independent parameters. Generally, its diagonal blocks $\Delta\mathsf{B}$ and $\Delta\mathsf{B}^{\perp}$, as well as its off-diagonal block $\Delta\mathsf{B}^{x}$, will be nonzero.

With this taken into consideration, the phase problem reduces to an optimization problem with respect to s, $\Delta\bar{\mathsf{B}}$ and the phases $\{\theta(\mathbf{Q})\}$. For example, we choose the least-squares-fit optimization*

$$\min_{s,\Delta\bar{\mathsf{B}},\{\theta(\mathbf{Q})\}}\sum_{\mathbf{Q}'}\Big|F^{p}_{\mathbf{Q}'}-s\sum_{\mathbf{Q}'^{\perp}}I_{\mathbf{Q}}^{1/2}\exp[i\theta(\mathbf{Q})+\bar{\mathbf{Q}}\Delta\bar{\mathsf{B}}\bar{\mathbf{Q}}]\Big|^{2}/N_{p}\sigma^{p}_{\mathbf{Q}'}\equiv R_{\rho}, \tag{4}$$

where N_p is the number of fitting points $\mathbf{Q}'$. The periodic crystal density F^{p} and the experimentally measured quasicrystal Bragg intensities $I_{\mathbf{Q}\neq0}$ are assumed known. By definition, $I_{\mathbf{Q}=0}\equiv(F_0/s\det\mathsf{L})^2$, where F_0 is the average (uniform) quasicrystal density, which can be assumed to be experimentally accessible. For $\sigma_{\mathbf{Q}'}$ we shall use $N_p^{-1}\sum_{\mathbf{Q}'}|F^{p}_{\mathbf{Q}'}|^2$, so that the resulting χ^2, denoted by R_ρ in (4), is analogous to the usual R factor used in crystallography. Here, it is a measure of the achieved closeness between the rational approximant and the periodic crystal.

The minimization with respect to the phases is simplified if the space-group symmetry of the quasiperiodic crystal is first specified. The diffraction pattern of a quasiperiodic crystal, in particular its point-group symmetry, is compatible only with a finite number of distinct space groups. Given a space group, phases at reciprocal-lattice vectors equivalent under the point-group symmetry, that is, phases on the same orbit, are uniquely determined by the phase of a *single* member of the orbit (Mermin, 1992). Furthermore, if the quasicrystal is centrosymmetric and the origin is chosen to coincide with the inversion center, the phases are restricted to 0 or π and the minimization in (4) is correspondingly simplified. For example, we shall use below this fact to perform the minimization numerically, using a program that determines the phases exactly by a complete enumeration.

The number N_p of orbits of the periodic crystal's Bragg peaks $F^{p}_{\mathbf{Q}'}$ that are to be fitted is related to the number N_q of orbits of measured quasiperiodic crystal peaks. Obviously, a peak $F^{p}_{\mathbf{Q}'}$ for which none of the quasiperiodic crystal peaks appearing in the sum in (2) is measured cannot be fitted and does not

* Different weighting and different methods, such as the maximum-entropy method, may be used instead. Also, following (3), $\Delta\mathsf{B}^{x}$ can be set to $\mathsf{E}^{\perp}\mathsf{L}^{-1}\cdot\mathsf{B}^{p}\bar{\mathsf{L}}^{-1}$.

Table 2. *Several Fourier transforms $F^p_{\mathbf{Q}'}$ of the scatterer densities in $R(Al_{0.564}Cu_{0.116}Li_{0.320})$ and the corresponding $F_{\mathbf{Q}} \exp(\bar{\mathbf{Q}}\Delta\mathsf{B}\bar{\mathbf{Q}})$ of $i(Al_{0.570}Cu_{0.108}Li_{0.322})$ for X-rays*

The numbers in parentheses are the multiplicities of the corresponding $\mathbf{Q}'$ orbits. Given a $\mathbf{Q}$ orbit, these numbers add up to the multiplicity of that orbit. Also shown are the measured intensities $I_{\mathbf{Q}}$, normalized to the largest measured intensity I_{max}.

(m)	$\mathbf{Q}'$	$F^p_{\mathbf{Q}'}$ ($\times 10^{-2}$ e Å^{-3})	$\bar{\mathbf{Q}}$	$I_{\mathbf{Q}}/I_{max}$	$F_{\mathbf{Q}} \exp(\bar{\mathbf{Q}}\Delta\mathsf{B}\bar{\mathbf{Q}})$ ($\times 10^{-2}$ e Å^{-3})
(12)	6 2 0	1.63	2 2 2 0 0 0	0.015	2.32
(8)	4 4 4	4.61	2 2 2 0 0 0	0.015	2.32
			2 2 2 1 $\bar{1}$ 1	0.031	−3.40
(12)	7 3 0	−6.77	2 2 2 1 $\bar{1}$ 1	0.031	−3.40
(12)	10 2 0	0.25	3 3 3 0 0 1	0.003	−1.11
(24)	7 7 2	0.18	3 3 3 0 0 1	0.003	−1.11
(24)	1 9 4	−3.13	3 3 3 0 0 1	0.003	−1.11
(24)	2 1 1	3.36	0 0 1 1 0 0	0.019	2.48
(6)	2 0 0	−0.38	0 0 1 1 0 0	0.019	2.48

appear in the sum in (4). It follows from dimension counting that, generically, $N_p \sim (N_q)^{3/D}$ as $N_q \to \infty$. Therefore, the number of unknown phases (N_q) grows much faster than the number of constraints (N_p) and (4) is generally insufficient to determine all the phases. Nevertheless, there are several reasons that the constraints expressed in (4) should often be sufficient in practice.

Typically, the point-group symmetry will be reduced in going from the quasiperiodic to the periodic crystal. Therefore, an orbit of peaks of the quasiperiodic crystal will generically split into $c = O_q/O_p$ orbits of peaks of the periodic crystal, where O_q and O_p are the orders of the two point groups (*e.g.* $O_q = |53m| = 120$ and $O_p = |m3| = 24$, resulting in $c = 5$). This means that a quasiperiodic crystal phase will be generally constrained by c equations. This, in turn, will often ensure that the system is overconstrained when N_q is not too large, allowing a unique solution of (4). Furthermore, as mentioned above, when the quasiperiodic crystal is centrosymmetric, the phases can be restricted to two values, 0 or π. Since, in such a case, several phases can be uniquely determined by a single constraint, the constraint counting is not applicable. We show explicitly in Table 2 splitting of the orbits and the resulting phases for several peaks of $i(Al_{0.570}Cu_{0.108}Li_{0.322})$, which will be used as an illustration below.

Finally, more than one periodic-crystal-rational-approximant pair may be known for a given quasiperiodic crystal, in which case each one provides an independent set of constraints. Then, a sum over all pairs can be included in (4) and a separate fitting parameter $\Delta\bar{\mathsf{B}}$ must be assigned to each pair. Clearly, as the increasingly weaker peaks are measured, the number of unknown phases N_q is increased and increasingly larger rational approximants will be needed for their accurate determination. While the phases associated with the strongest peaks can be well constrained even with a small rational approximant, the uncertainty in the phases associated with the weakest measurable peaks may become quite large. In particular, peaks at the smallest $\mathbf{Q}$ have the largest $\mathbf{Q}^{\perp}$ and will typically be the weakest. This means that the density of the quasiperiodic crystal determined with our method will be least reliable on the scales much larger than the unit cell of the used rational approximant.

Once the scale, s, which includes such factors as $(\det \mathsf{L})^{-1}$ and $N^{-1/2}$, is determined by our method, the resulting quasiperiodic crystal density,

$$F_{\mathbf{Q}} = s \det \mathsf{L} I_{\mathbf{Q}}^{1/2} \exp[i\theta(\mathbf{Q})], \qquad (5)$$

is obtained in absolute units. Different data sets for the same quasiperiodic compound could result not only in different s but also in a different $\Delta\bar{\mathsf{B}}$, even when the reference periodic crystal is the same. For example, the two sets could be taken at two different temperatures. Then, for the purpose of a comparison, the density in (5) could be multiplied by the appropriate Debye–Waller correction factors.

Tests

The applicability of our method cannot be established *a priori* for each periodic-crystal–rational-approximant pair. However, the best results can be expected when the required distortions are small ($\mathsf{E}^{\perp} \ll l_{\perp}/l$ and $\mathsf{L} \simeq 1$) and when the density, stoichiometry and local environments in the quasiperiodic and periodic crystals are similar. This is exemplified when $D = 3$ so that quasiperiodicity reduces to periodicity. Then, a rational approximant of the ('quasi')periodic crystal is another periodic crystal and to each reciprocal-lattice vector $\mathbf{Q}'$ corresponds a *unique* reciprocal-lattice vector $\mathbf{Q}$ with the same Miller indices. Therefore, a real periodic crystal that is to be identified with the approximant must have the identical stoichiometry and differ only by atomic displacements within the unit cell. In the limit $\mathsf{L} \to 1$, the characteristic shift Δr of the atomic positions will be small if the local environments in the two crystals are similar. Thus, the error in the phase $\theta(\mathbf{Q})$ obtained using our method, which is on the order of $Q\Delta r$, will also be small for experimentally accessible Q values.

For the general case when $D>3$, it is instructive first to examine the effects of the truncation of the sum in (2). We wish to determine the accuracy of the answers obtained with our method in cases when the quasiperiodic density is explicitly given and the periodic crystal and a rational approximant are identical, except for the presence of the Debye–Waller factor $\exp(-\mathbf{Q}^{\perp}\mathsf{B}^{\perp}\mathbf{Q}^{\perp})$ in the rational approximant. Ideally, we should recover all phases correctly, $s=1$ and $\Delta\mathsf{B}$ as given by (3). Below, we present the main results of an example analyzed in greater detail elsewhere (Jarić & Qiu, 1992).

We consider quasiperiodic icosahedrally symmetric densities associated with perfect and random Ammann tilings (Mackay, 1981; Tang, 1991). Point-like scatterers are placed at the vertices of the tilings, resulting in the space-group symmetry $P53m$. This symmetry restricts the phases to 0 or π and forces all phases on a single orbit to be identical (Mermin, 1992). Here, the reciprocal lattice $\{\mathbf{Q}\}$ is generated by $D=6$ equal-length vectors along the six five-fold axes of an icosahedron. The associated hypercrystal is simple cubic. In both cases, $F_{\mathbf{Q}}\sim t(\mathbf{Q}^{\perp})\exp(-\mathsf{B}^{\perp}|\mathbf{Q}^{\perp}|^2)$, where $t(\mathbf{Q}^{\perp})$ is the Fourier transform of a rhombic triacontahedron in the inner space (Elser, 1985*b*).

The inner-space Debye–Waller factors differ in the two cases, with $\mathsf{B}^{\perp}_{\text{perfect}}=0$ and $\mathsf{B}^{\perp}_{\text{random}}=0.0833$, both scalars by symmetry. The second value is obtained from computer simulations (Tang, 1991). Our periodic crystal is the b.c.c. rational approximant obtained with $\mathsf{E}^{\perp}=[(1+5^{1/2})/2]^{-3}$ and $\mathsf{L}=1$, which are both scalars in the coordinate system of Jarić (1986, 1987). For the sake of completeness, we also include in all densities a Debye–Waller factor $\exp(-Q^2/2400)$ corresponding to the r.m.s. fluctuations of the atoms in the physical space equal to 5% of the tile edge length. This also fixes $\Delta\mathsf{B}^{x}\equiv\mathsf{E}^{\perp}\mathsf{L}^{-1}\mathsf{B}^{p}\tilde{\mathsf{L}}^{-1}\simeq 9.8\times10^{-5}$.

By taking a scattering intensity cut-off at 0.1% of the maximum intensity, we obtain 402 independent measurable intensities for the perfect tiling. We recover 397 phases correctly with the relatively low resulting $R_\rho=0.0496$. For the scale, we find $s=0.9(2)$, while for the Debye–Waller corrections we get $\Delta\mathsf{B}^{\perp}=0.01(3)$ for the inner space and $\Delta\mathsf{B}=0.0(8)\times10^{-4}$ for the physical space. These values compare favorably with the correct values $s=1$, $\Delta\mathsf{B}^{\perp}=0$ and $\Delta\mathsf{B}=0$, provided that the two Debye–Waller corrections are expressed in appropriate units ($l_{\perp}^2=5.332$ and $l^2=0.750$, respectively).

The 0.1% cut-off leads to 229 independent measurable intensities for the random tiling. Now, we recover all their phases correctly and obtain a low $R_\rho=0.00195$. Although the obtained value for $\Delta\mathsf{B}$ [$0.0(3)\times10^{-4}$] is as close to the correct value $\Delta\mathsf{B}=0$ as it was in the case of perfect tiling, the scale $s=0.79(8)$ and $\Delta\mathsf{B}^{\perp}=0.15(2)$ are not as close to their correct values, $s=1$ and $\Delta\mathsf{B}^{\perp}=0.0833$. The reason is that $\mathsf{B}^{\perp}=0.0833$ is so large that only one term is above the cut-off in the sums in (2). When expressed in appropriate units, this $\mathsf{B}^{\perp}$ is at least five times larger than what is obtained in the next section for $i(Al_{0.570}Cu_{0.108}Li_{0.322})$.* Indeed, if we reduce $\mathsf{B}^{\perp}$ to 0.0417, increasing the number of measurable intensities to 288, we recover all but one of the phases correctly. We also obtain much better values for s [$=0.9(1)$], $\Delta\mathsf{B}^{\perp}$ [$=0.05(2)$; the correct value is 0.0417] and $\Delta\mathsf{B}$ [$=0.0(4)\times10^{-4}$], resulting in a still excellent $R_\rho=0.0296$. Further discussion of the intensity cut-off effects on the reconstruction is provided by Jarić & Qiu (1992), Qiu & Jarić (1992) and Qiu (1992).

Application to $i(Al_{0.570}Cu_{0.108}Li_{0.322})$

As an illustration, we now apply our method to the X-ray and neutron scattering data of the icosahedral quasicrystal $i(Al_{0.570}Cu_{0.108}Li_{0.322})$ obtained by de Boissieu *et al.* (1991). The data contain $N_q=56$ and 40 independent peaks for X-rays and neutrons, respectively. The assumption that the quasicrystal density is well approximated by a quasiperiodic density is supported by several observations. (i) The quasicrystal diffraction peaks can be indexed to within 10^{-3} Å^{-1} with the icosahedral reciprocal lattice described above for the Ammann tilings with the $D=6$ hypercubic lattice constant $\bar{a}=7.15$ Å. (ii) The coherence length in the quasicrystal is not too short, on the order of 1000 Å. (iii) The associated quasiperiodic Patterson function of the quasicrystal is extremely simple when viewed as a periodic function in the hyperspace, which could hardly be a coincidence (Qiu & Jarić, 1989; de Boissieu *et al.*, 1991; van Smaalen, de Boer & Shen, 1991).

We take the b.c.c. $R(Al_{0.564}Cu_{0.116}Li_{0.320})$ as the related periodic crystal since it is close to $i(Al_{0.570}Cu_{0.108}Li_{0.322})$ both in stoichiometry and density (2.46 g cm^{-3} *vs* 2.47 g cm^{-3}) and it has similar local environments (Elser & Henley, 1985). Its structure has been refined recently by Audier *et al.* (1988). Indeed, we find that the same distortion we used for the Ammann tilings, $\mathsf{E}^{\perp}\simeq0.236$, and a small compression $\mathsf{L}=0.999$ produce a b.c.c. rational approximant with the same lattice constant $a=13.91$ Å as observed in $R(Al_{0.564}Cu_{0.116}Li_{0.320})$. The strain $\mathsf{E}^{\perp}$ is quite small, about 3%, when expressed in its natural units of $l_{\perp}/l$. The values $l\simeq2.549$ Å and $l_{\perp}\simeq20.05$ Å can be determined easily from the known density and stoichiometry of $i(Al_{0.570}Cu_{0.108}Li_{0.322})$.

No other periodic crystals need to be considered to determine the phases if we assume that the

* The comparison can be made either with $l_{\perp}$ as the unit of length in the inner space or with a decorated Ammann tiling model of $i(Al_{0.570}Cu_{0.108}Li_{0.322})$, such as the model by van Smaalen, de Boer & Shen (1991). It also depends on whether X-ray or neutron data are used.

quasiperiodic crystal has the primitive space-group symmetry $P53m$ (Mermin, 1992), which is consistent with the diffraction pattern and with the space group $Im3$ of $R(Al_{0.564}Cu_{0.116}Li_{0.320})$. Then the hypercrystal is centrosymmetric, which restricts the phases to 0 or π and reduces the number of necessary constraints.* Moreover, the phases are overconstrained, on the average, with $N_p/N_q = 157/56 \simeq 2.8$ and $107/40 \simeq 2.7$ constraints per phase for the X-ray and neutron data, respectively.

As we mentioned earlier, distortions of the hypercrystal below its unit-cell scale may be necessary in addition to the overall linear distortion L. To compensate for such distortions, before proceeding with the minimization in (4), we first slightly adjust the atomic coordinates of $R(Al_{0.564}Cu_{0.116}Li_{0.320})$ so that they coincide with the special positions when imbedded into the hypercrystal (Yamamoto, 1990). This is motivated by the observation that the quasiperiodic Patterson function of $i(Al_{0.570}Cu_{0.108}Li_{0.322})$ has dominant contributions associated with these positions (Qiu & Jarić, 1989; de Boissieu *et al.*, 1991; van Smaalen, de Boer & Shen, 1991). This adjustment has a very small effect on the resulting $F_{\mathbf{Q}}$: all the phases remain the same for the neutron data while only the phase associated with the second-weakest intensity [the (3 3 3 0 0 1) orbit in Tables 1 and 2] changes for the X-ray data. Hereafter, we shall consider only the adjusted structure of $R(Al_{0.564}Cu_{0.116}Li_{0.320})$.

The Fourier components $F_{\mathbf{Q}}$ resulting from the minimization are given in Table 1. The associated phases can be simply read from the sign of $F_{\mathbf{Q}}$. The other fitted parameters are $\Delta B = 0.0061(1)$ Å^2, $\Delta B^{\perp} = 0.018(1)$ Å^2 and $s = 1.771(1) \times 10^{-2}$ e Å^{-3}, for X-rays. For neutrons, $\Delta B = 0.0046(2)$ Å^2, $\Delta B^{\perp} = 0.39(4)$ Å^2 and $s = 7.43(8)10^{-8}$ Å^{-2}. The values $\Delta B^{x} = 0.0015$ Å^2 and 0.0018 Å^2 were fixed for X-rays and neutrons, respectively, using (3) and $B^{p} = 0.0063$ Å^2 and 0.0071 Å^2, respectively, deduced from Audier *et al.* (1988). We show in Table 2 the only cases we found where phases were overconstrained with mutually inconsistent constraints. All of them correspond to very weak peaks.

For example, consider the single orbit of 60 $i(Al_{0.570}Cu_{0.108}Li_{0.322})$ peaks represented by $\mathbf{Q} = (3\,3\,3\,0\,0\,1)$. It splits into three $R(Al_{0.564}Cu_{0.116}Li_{0.320})$ orbits of 12, 24 and 24 peaks each, represented by $\mathbf{Q}' = (10\,2\,0)$, $(7\,7\,2)$ and $(1\,9\,4)$, respectively. The first two orbits, $(10\,2\,0)$ and $(7\,7\,2)$, require that $\theta(3\,3\,3\,0\,0\,1) = 0$, while the third orbit requires it to be π. Indeed, the third orbit forces the optimal solution to be π since it is the largest orbit and the corresponding $|F^{p}_{\mathbf{Q}'}|$ is the largest. Other cases shown in Table 2 can be understood similarly.

The R_p values corresponding to the optimal solutions listed in Table 1 are $R_p^{\text{X-ray}} = 0.0543$ and $R_p^{\text{neutron}} = 0.0383$. These values can be best assessed by comparison of the resulting three-dimensional density maps obtained for the rational approximant corrected for $\Delta\bar{B}$ with those obtained for $R(Al_{0.564}Cu_{0.116}Li_{0.320})$ using the same Fourier components. The agreement shown in Fig. 3 is excellent. Each shown isodensity surface surrounds a high-density region, typically centered at an ideal (equilibrium) atomic position in the structure model of $R(Al_{0.564}Cu_{0.116}Li_{0.320})$. The rational approximant isodensity surfaces are nearly identical with the $R(Al_{0.564}Cu_{0.116}Li_{0.320})$ surfaces for both X-rays and neutrons.

With the results given in Table 1, we can also calculate the associated quasiperiodic $i(Al_{0.570}Cu_{0.108}Li_{0.322})$ density. As anticipated, it exhibits some icosahedral local environments similar to the ones found in the $R(Al_{0.564}Cu_{0.116}Li_{0.320})$ crystal. This is clearly seen by comparison of the density maps in Figs. 1(*a*) and 3(*a*) for X-rays [in addition to a surface at the center, the surfaces in Fig. 1(*a*) are located at vertices of two nested icosahedra]. The only significant differences, seen in the shape of the neutron data isodensity surfaces in Figs. 1(*d*) and 3(*c*), are caused by the approximate nature of the icosahedral symmetry in the b.c.c. crystal. Clearly, $i(Al_{0.570}Cu_{0.108}Li_{0.322})$ may also contain local environments that are not present in $R(Al_{0.565}Cu_{0.116}Li_{0.320})$. Examples are the fivefold symmetric environments in Figs. 1(*b*) and (*e*), and the icosahedral ones in Figs. 1(*c*) and (*f*). The reader is encouraged to identify in Fig. 1(*b*) the nearly vertical fivefold symmetry axis (passing through three surfaces) and a series of perpendicular pentagons with surfaces at their vertices. Similarly, the 80 surfaces in Fig. 1(*c*) can be connected to form hexagons and pentagons covering a sphere in an icosahedrally symmetric fashion.

The resulting quasicrystal density becomes very simple when viewed as periodic six-dimensional simple-cubic density. By examining high-symmetry planes through high-symmetry points, such as the threefold symmetry plane through a vertex of the hypercubic lattice shown in Fig. 2(*a*), we find that the density is concentrated in the three-dimensional planes parallel to the inner space and centered at vertices, edges centers and body centers of the hypercubic lattice. Constant-density surfaces in these three-dimensional planes are shown in Fig. 4. They are related to the physical-space structures, shown in Fig. 1, which are also centered at vertices (*a*, *c*), edge centers (*b*, *e*), and body centers (*c*, *f*). An understanding of the atomic density in the inner space is very important for the modeling of the ideal atomic structure of the quasiperiodic crystal (Qiu, 1992).

* Since the phases depend on the position of the origin, the restriction of the phases to 0 or π requires that the origin be fixed at a $53m$ symmetry center in the hypercrystal, which, in turn, must coincide with an $m3$ symmetry center in the approximant. Furthermore, for the X-ray data, the anomalous dispersion must be neglected.

The surfaces that can be seen in the neutron data that are absent from the X-ray data correspond to the negative density $\rho = -3.17 \times 10^{-5}$ Å^{-2} coming from the hypercubic body center. This is consistent with the assumption that the body-center density is dominated by Li, which is a weak X-ray scatterer and has a negative neutron scattering length. On the other hand, the positive density, centered at vertices or edge centers, is probably dominated by Al and Cu. Further analysis, including more extensive X-ray data (van Smaalen, de Boer & Shen, 1991) and implications of our results to the structural modeling of $i(Al_{0.570}Cu_{0.108}Li_{0.322})$ are presented elsewhere (Qiu & Jarić, 1992; Qiu, 1992).

Concluding remarks

We have presented a general method to solve the phase problem in a class of quasiperiodic crystals for which related periodic crystals of known structure exist. This method enables one to reconstruct the density of scatterers, which is important in understanding the physical properties of a material and can also be used as a guide in determining the 'ideal' atomic structure of the material, whenever this concept is meaningful. The method reproduced the correct phases for the perfect and random tiling models we considered. Its application to $i(Al_{0.570}Cu_{0.108}Li_{0.322})$ resulted in a reasonable quasiperiodic density and phases in good agreement with the result of two recent structure models (de Boisseau *et al.*, 1989, 1991), the only structure models based on the same diffraction data we used here (de Boissieu *et al.*, 1991). However, a detailed analysis of the calculated density and its implications for the structure modeling are beyond the scope of this article and will be presented elsewhere. Systems where this method may prove particularly valuable are the usual incommensurate crystals that can be related to a periodic crystal by a small displacive reconstruction in the physical space.

We thank G. Vallis for access to his 3D visualization equipment, S. Johnson and M. Maltrud for computer assistance and G. Agnolet and Y. Kantor for useful comments. One of us (MVJ) is grateful to colleagues in the Physics Department and the Institute of Nonlinear Science at University of California, Santa Cruz,

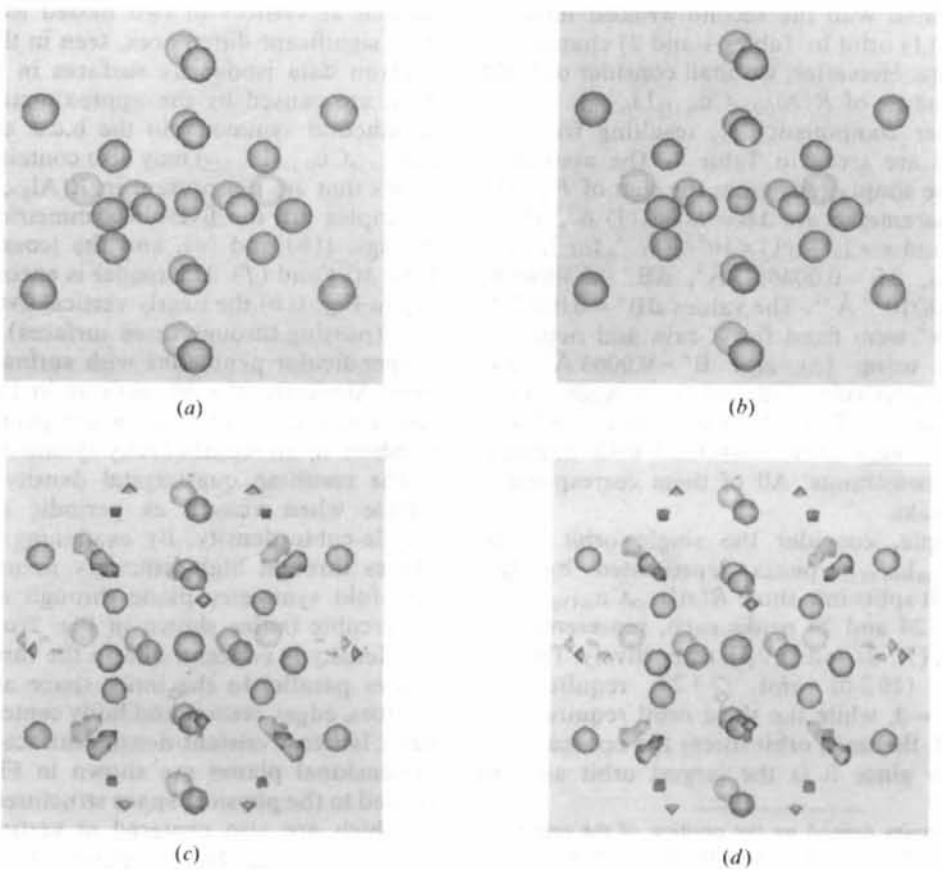

Fig. 3. Surfaces of constant scatterer density of $R(Al_{0.564}Cu_{0.116}Li_{0.320})$ (*a*), (*b*) and a rational approximant to $i(Al_{0.570}Cu_{0.108}Li_{0.322})$ (*b*), (*d*). The density is 11.9e Å^{-3} for X-rays (*a*), (*b*) and -3.17×10^{-5} Å^{-2} or 7.39×10^{-5} Å^{-2} for neutrons (*c*), (*d*). Densities within a sphere of radius 5.6 Å centered at $m3$ symmetry points are shown, revealing an approximate $53m$ symmetry.

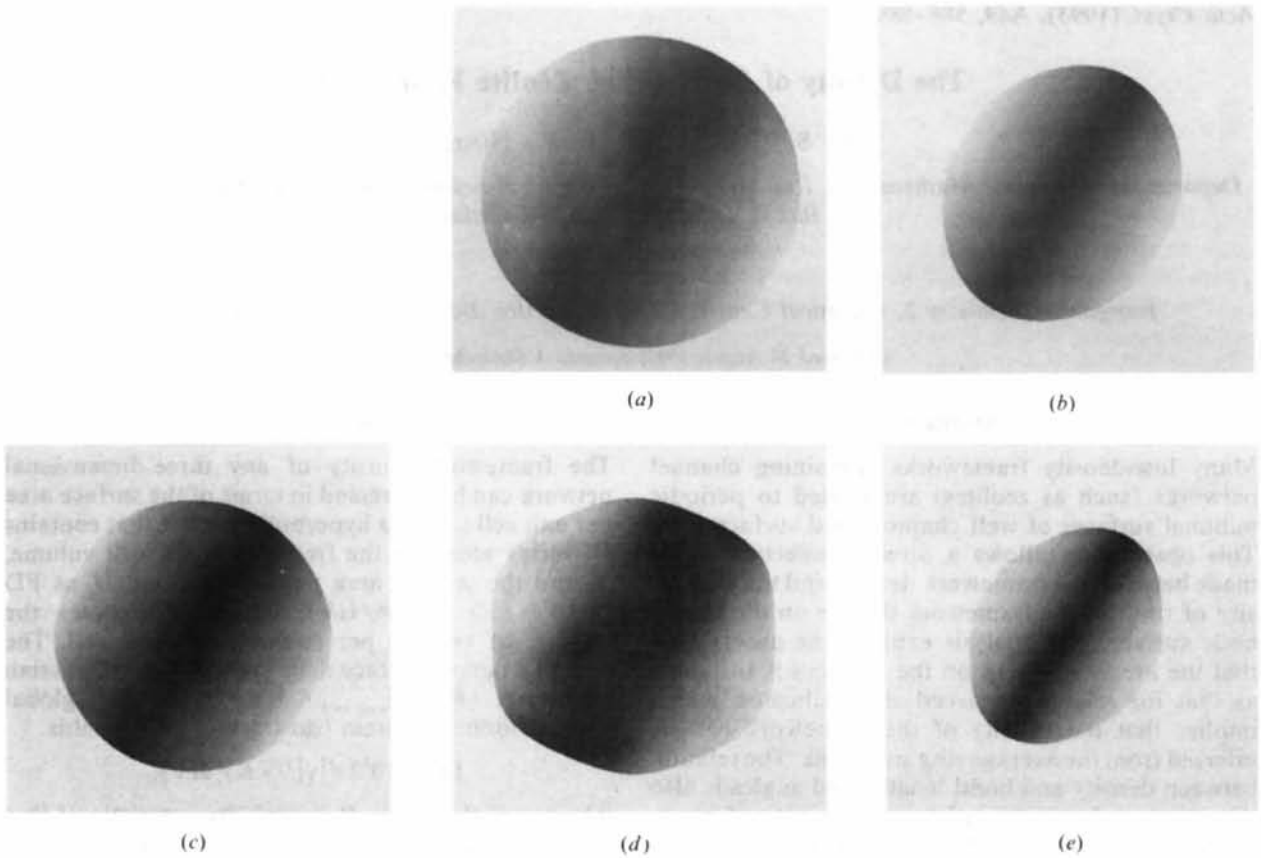

Fig. 4. Surfaces of constant scatterer density in the inner space. The density is 7.39×10^{-5} Å^{-2} (a), (b) or -3.17×10^{-5} Å^{-2} (c) for neutrons. For X-rays, it is 11.9e Å^{-3} (d), (e). The densities are shown within cubes of edge 20 Å centered at vertices (a), (c), edge centers (b), (d) and a body center (e) of the hypercubic lattice. Their symmetries are $53m$, $\bar{5}m$ and $53m$, respectively. Two light sources are located at opposite ends of a fivefold symmetry axis.

for hospitality and support and he dedicates this work to Michelle, Nicholas and Kyle whose love made it possible. This work was funded in part by the NSF grant No. DMR8821802.

References

AUDIER, M., PANNETIER, J., LEBLANC, M., JANOT, C., LANG, J.-M. & DUBOST, B. (1988). *Physica (Utrecht)*, **B153**, 136–142.
BAK, P. (1986). *Scr. Metall.* **20**, 1199–1204.
BESICOVITCH, A. S. (1932). *Almost Periodic Functions.* Cambridge Univ. Press.
BOHR, H. A. (1947). *Almost Periodic Functions.* New York: Chelsea Publishing.
BOISSIEU, M. DE, JANOT, C., DUBOIS, J. M., AUDIER, M. & DUBOST, B. (1991). *J. Phys. Condens. Matter*, **3**, 1–25.
BOISSIEU, M. DE, JANOT, C., DUBOIS, J. M., AUDIER, M., JARIĆ, M. & DUBOST, B. (1989). *Quasicrystals*, edited by M. V. JARIĆ & S. LUNDQVIST, pp. 109–129. Singapore: World Scientific.
CAHN, J. W., SHECHTMAN, D. & GRATIAS, D. (1986). *J. Mater. Res.* **1**, 13–26.
ELSER, V. (1985*a*). *Phys. Rev. Lett.* **54**, 1730.
ELSER, V. (1985*b*). *Phys. Rev. B*, **32**, 4892–4898.
ELSER, V. & HENLEY, C. L. (1985). *Phys. Rev. Lett.* **55**, 2883–2886.
HAUPTMAN, H. (1986). *Science*, **233**, 178–183.
JARIĆ, M. V. (1986). *J. Phys. (Paris)*, **C3-47**, 82–83.
JARIĆ, M. V. (1987). *Group Theoretical Methods in Physics*, edited by R. GILMORE, pp. 288–293. Singapore: World Scientific.
JARIĆ, M. V. & MOHANTY, U. (1987). *Phys. Rev. Lett.* **58**, 230–233.
JARIĆ, M. V. & NELSON, D. R. (1988). *Phys. Rev. B*, **37**, 4458–4472.
JARIĆ, M. V. & QIU, S.-Y. (1990). *Quasicrystals*, edited by T. FUJIWARA & T. OGAWA, pp. 48–56. Berlin: Springer-Verlag.
JARIĆ, M. V. & QIU, S.-Y. (1991). *Methods of Structural Analysis of Modulated Structures and Quasicrystals*, edited by J. M. PÉREZ-MATO, F. J. ZÚÑIGA & G. MADARIAGA, pp. 481–491. Singapore: World Scientific.
JARIĆ, M. V. & QIU, S.-Y. (1992). *J. Non-Cryst. Solids.* In the press.
KARLE, J. (1986). *Science*, **232**, 837–843.
MACKAY, A. L. (1981). *Sov. Phys. Crystallogr.* **26**, 517–522.
MERMIN, D. (1992). *J. Mod. Phys.* **64**, 3–49.
QIU, S.-Y. (1992). PhD thesis, Texas A&M Univ., USA.
QIU, S.-Y. & JARIĆ, M. V. (1989). *Quasicrystals*, edited by M. V. JARIĆ & S. LUNDQVIST, pp. 19–33. Singapore: World Scientific.
QIU, S.-Y. & JARIĆ, M. V. (1990). *Quasicrystals and Incommensurate Structures in Condensed Matter*, edited by M. J. YACAMÁN, D. ROMEU, V. CASTAÑO, & A. GÓMEZ, pp. 170–179. Singapore: World Scientific.
QIU, S.-Y. & JARIĆ, M. V. (1992). *J. Non-Cryst. Solids.* In the press.
SMAALEN, S. VAN, DE BOER, J. L. & SHEN, Y. (1991). *Phys. Rev. B*, **43**, 929–937.
STEINHARDT, P. J. & OSTLUND, S. (1987). *The Physics of Quasicrystals.* Singapore: World Scientific.
TANG, L.-T. (1991). *Phys. Rev. Lett.* **64**, 2390–2393.
YAMAMOTO, A. (1990). *Quasicrystals*, edited by T. FUJIWARA & T. OGAWA, pp. 57–67. Berlin: Springer-Verlag.